Motion-induced synchronization in metapopulations of mobile agents

Jesús Gómez-Gardeñes,[1,2,*] Vincenzo Nicosia,[3,4,*] Roberta Sinatra,[5] and Vito Latora[3,6]

[1]*Departamento de Física de la Materia Condensada, University of Zaragoza, Zaragoza 50009, Spain*

[2]*Institute for Biocomputation and Physics of Complex Systems (BIFI), University of Zaragoza, Zaragoza 50018, Spain*

[3]*School of Mathematical Sciences, Queen Mary University of London, London E1 4NS, United Kingdom*

[4]*Computer Laboratory, University of Cambridge, Cambridge CB3 0FD, United Kingdom*

[5]*Center for Complex Network Research and Department of Physics, Northeastern University, Boston, Massachusetts 02115, USA*

[6]*Dipartimento di Fisica e Astronomia, Università di Catania and INFN, 95123 Catania, Italy*

(Received 9 June 2012; revised manuscript received 15 October 2012; published 28 March 2013)

We study the influence of motion on the emergence of synchronization in a metapopulation of random walkers moving on a heterogeneous network and subject to Kuramoto interactions at the network nodes. We discover a mechanism of transition to macroscopic dynamical order induced by the walkers' motion. Furthermore, we observe two different microscopic paths to synchronization: depending on the rule of the motion, either low-degree nodes or the hubs drive the whole system towards synchronization. We provide analytical arguments to understand these results.

DOI: 10.1103/PhysRevE.87.032814 PACS number(s): 89.75.Hc, 05.45.Xt

I. INTRODUCTION

The spontaneous emergence of synchronization in systems of coupled dynamical units [1,2] underlies the development of coordinated tasks as diverse as metabolic cycles in eukaryote cells, cognitive processes in the human brain, and opinion formation in social systems [3–6]. In the last decade complex networks theory has revealed that the topology of the interactions in a complex system has important effects on its collective behavior [7,8]. As a consequence, many recent studies have considered dynamical systems coupled through nontrivial topologies [9], uncovering the impact of the structure of the network on the existence [10–14] and stability [15–18] of synchronized states.

Quite frequently, the interactions among the units of a complex system keep changing over time. Their evolution can either be driven by the synchronization process itself, as in models of co-evolving networks [19–22], or be determined by the fact that each unit moves at random over a continuous and homogeneous space and interacts only with other units within a given distance [23–27].

In many cases, the motion of the agents takes place on discrete and heterogeneous media that can be represented as complex networks. Typical examples include users browsing the World Wide Web, airplane passengers traveling throughout a country, or people playing online social games [28–30]. In such systems, both the rule of motion adopted by the agents, and the heterogeneity of the environment, have an impact on the emergence and stability of collective behaviors. For this reason, metapopulation modeling has been successfully employed to explore the combined effect of mobility and nontrivial interaction patterns in different contexts, including the study of epidemic spreading and chemical reactions [28,29,31–34].

In this work we propose a metapopulation model to study the emergence of synchronization in populations of individuals moving over discrete heterogeneous environments and interacting through nonlinear dynamical equations. We assume that each agent is characterized by an internal state (or opinion) and that it moves over the environment trying to synchronize its opinion with that of the other individuals. Thus, the evolution of the system is driven by the interplay of two concurrent processes: On one hand, the interaction of neighboring agents drives their internal state towards local consensus; on the other hand, the agents' motion dynamically changes the pattern of interaction and allows each agent to be exposed to different opinions. We discover a novel mechanism of synchronization that we name *motion-induced synchronization* since the transition from disorder to macroscopic order is controlled by the value of the parameter tuning the motion of the agents. Furthermore, we show that there are two different microscopic mechanisms driving the system towards synchronization, according to whether the walkers prefer to visit or to avoid high-degree nodes.

II. MODEL

Our metapopulation model consists of two layers. At the bottom layer we have a set of W mobile agents (walkers). Each agent i ($i = 1,2,\ldots W$) is a dynamical system whose internal state at time t is described by a phase variable $\theta_i(t) \in [0,2\pi)$, and changes over time as a result of the interactions with other agents. The top layer consists of a complex network with N nodes and E edges, which represents the environment into which the agents interact (nodes) and move (edges). The network is described by an adjacency matrix $\mathcal{A}$, whose entry a_{IJ} is equal to 1 if nodes I and J are connected by an edge and 0 otherwise (here and in the following we indicate nodes of the graph in uppercase letters and walkers in lowercase).

At any given time, each agent is located in one of the nodes of the network. The agent interacts for a fixed time interval with other agents at the same node, trying to synchronize its phase with the others' phase. Then, it moves to one of the neighboring nodes, chosen according to a one-parameter motion rule. More precisely, assume that at time t we have $i \in I$, i.e., agent i is at node I. The evolution of the phase $\theta_i(t)$ of agent i is ruled by an all-to-all Kuramoto-like interaction with the other walkers

[*] J.G.G. and V.N. contributed equally to this work.

being on the same node I at time t [3,35,36]

$$\dot{\theta}_i(t) = \omega_i + \lambda \sum_{j \in I} \sin[\theta_j(t) - \theta_i(t)] , \quad \forall i \in I, \tag{1}$$

where ω_i is the internal frequency of agent i and λ is a control parameter accounting for the strength of the interaction among walkers. Notice that, when the phases of the agents evolve according to Eq. (1), the system is not driven by a single global mean field (as in the classical all-to-all Kuramoto model). Instead, each oscillator i interacts with the *local* mean-field phase due to all the oscillators being at the same node as i.

At regular time intervals of length Δ all the agents perform one step of a *degree-biased* random walk on the network. Namely, we assume that a walker at node I moves to a neighboring node J with a probability proportional to the degree k_J of the destination node [37,38]

$$\Pi_{I \to J} = \frac{a_{IJ} k_J^{\alpha}}{\sum_{L=1}^{N} a_{IL} k_L^{\alpha}} . \tag{2}$$

Here α is a tunable parameter which biases the agents' motion either towards low-degree nodes ($\alpha < 0$) or towards hubs ($\alpha > 0$). For $\alpha = 0$, we recover the standard (unbiased) random walk. In summary, the metapopulation model has three control parameters: λ regulating the interaction strength among walkers, α tuning the rule of their motion, and Δ fixing the ratio between the time scales of interaction and motion.

The degree of synchronization of the whole metapopulation at time t is measured by the global order parameter

$$r(t) = \left| \frac{1}{W} \sum_{i=1}^{W} e^{i\theta_i(t)} \right|, \tag{3}$$

where $r \simeq 0$ if the phases of the agents are completely incoherent, while $r = 1$ when the system is fully synchronized. To quantify the degree of synchronization of a single node I we introduce the local order parameter

$$r_I(t) = \left| \frac{1}{w_I(t)} \sum_{i \in I} e^{i\theta_i(t)} \right| , \quad I = 1,2,\ldots,N, \tag{4}$$

where $w_I(t)$ is the number of agents at node I at time t. When the phases of the walkers at node I are fully synchronized, the local order parameter of the node is equal to 1, while in the case of complete local disorder we have $r_I(t) = 0$. We can also quantify the average local synchronization of the network $r_{\rm loc}(t)$ as the average of $r_I(t)$ over all nodes, i.e.,

$$r_{\rm loc}(t) = \frac{1}{N} \sum_{I} r_I(t). \tag{5}$$

We notice that, having $r_I(t) \simeq 1 \; \forall I$, or equivalently, $r_{\rm loc}(t) \simeq 1$ is a necessary but not sufficient condition to attain global synchronization. In fact, in the limiting case in which there is no motion ($\Delta \to \infty$) and λ is large enough, it is possible to have $r_I(t) \simeq 1 \; \forall I$ and, at the same time, $r(t) \simeq 0$.

III. RESULTS

We have simulated the metapopulation model on various synthetic networks and, as an example of a real complex network, on the U.S. air-transportation system, which includes the flight connections between the $N = 500$ largest airports in the U.S. Thanks to its intrinsic nature as a backbone for human transportation, the U.S. airports' network has already been used to investigate reaction-diffusion dynamics in metapopulation models [28]. This network has a long-tailed degree distribution, exhibits degree-degree correlations, and is relevant for the present study because opinion formation in real social systems is often mediated by information, communication, and transportation networks having similar structural properties. We have generated, for comparison, uncorrelated scale-free (SF) networks with $N = 500$ nodes and a power-law degree distribution $P(k) \sim k^{-\gamma}$ with a tunable value of the exponent γ [39].

For the numerical simulations of the model, the initial phases of the oscillators have been sampled uniformly in $[0,2\pi)$, and their internal frequencies ω_i from a uniform distribution $g(\omega) = 1/2 \; \forall \; \omega \in [-1,1]$. We started from a stationary distribution of $W = 5000$ walkers over the network [37], and we integrated Eq. (1) for all the agents for a time $t_0 = m\Delta$, where $m = 10^4$ is the number of random walk steps performed. After this transient, we estimated global and local synchronization parameters (r, $r_{\rm loc}$, and r_I for $I = 1,\ldots,N$) by respectively averaging the values obtained from Eqs. (3), (4), and (5) over a time window of length $T = 2m\Delta$.

A. Synchronization transition

In Fig. 1 we show the global order parameter r as a function of the coupling strength λ and of the walker bias α. The three phase diagrams have been obtained setting $\Delta = 0.05$, but qualitatively similar results have been obtained for different values of Δ. The SF networks reported in Figs. 1(a) and 1(b) have, respectively, $\gamma = 2.7$ and $\gamma = 3$. As expected, by increasing λ at a fixed value of α, i.e., keeping fixed the rules of motion, we observe a phase transition from the incoherent phase ($r \simeq 0$, dark regions of the diagrams) to a synchronized state ($r \neq 0$, bright regions of the diagrams). However, the precise value for the onset of synchronization, namely the critical value λ_c for which the incoherent state becomes unstable, strongly depends on the motion bias α. In particular, we find that $\lambda_c(\alpha)$ is first increasing as a function of α and then decreasing. The function $\lambda_c(\alpha)$ reaches its maximum $\lambda_c^{\max}$ at a particular value of α, namely at $\alpha^* \simeq -0.5$ for the air-transportation network and at $\alpha^* \simeq -1$ for the two SF networks. By comparing the diagrams obtained for the two SF networks we also observe that, for any value of α, the critical value of λ_c is smaller for SF networks with $\gamma = 2.7$ [Fig. 1(a)] than for those having $\gamma = 3.0$ [Fig. 1(b)], thus confirming that degree heterogeneity tends to favor global synchronization.

As a consequence of the shape of $\lambda_c(\alpha)$, for a wide range of values of the strength λ such that $\lambda < \lambda_c^{\max}$, we observe a novel mechanism of *motion-induced* synchronization. This means that we can fix the value of the interaction strength λ, and we can control whether the system is in the incoherent phase ($r \simeq 0$, dark regions) or in the synchronized state ($r \neq 0$, bright regions) solely by changing the rule of motion.

Let us focus on the case of the SF network shown in Fig. 1(b) and suppose to keep λ fixed at 0.08 (see the horizontal line in the figure). As shown in Fig. 1(d), we can start with a value

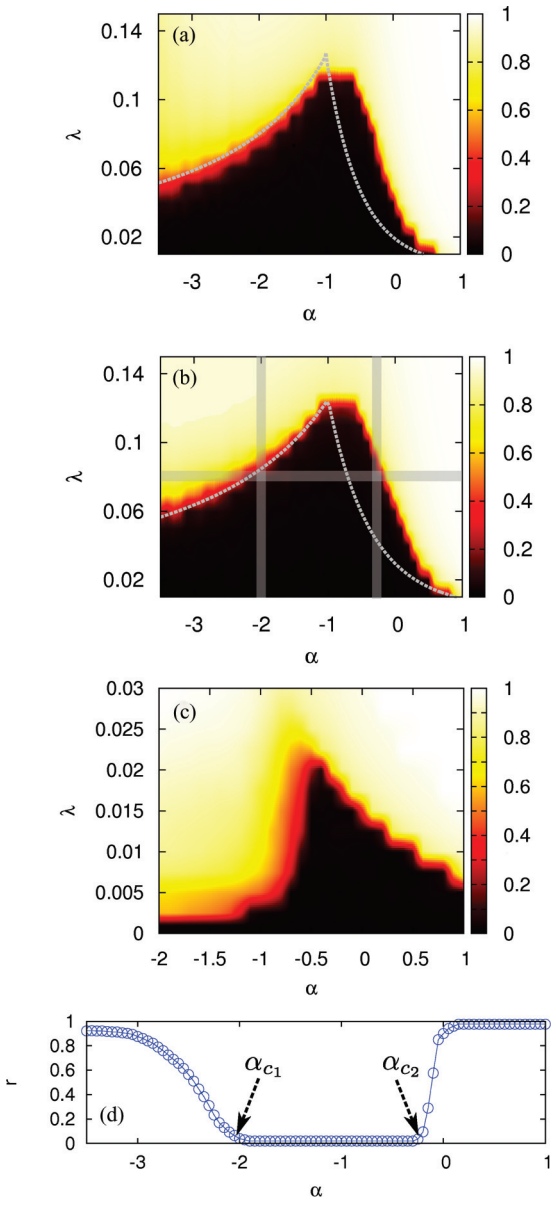

FIG. 1. (Color online) Phase diagram $r(\alpha,\lambda)$ of the metapopulation model on uncorrelated SF networks with (a) $\gamma = 2.7$, (b) $\gamma = 3.0$, and (c) on the U.S. air-transportation network. The three networks have $N = 500$ nodes. The dashed curves in panels (a) and (b) are the corresponding lower-bound analytical predictions for the onset of synchronization in uncorrelated graphs obtained from Eq. (9) for $\alpha > -1$, and from Eq. (10) for $\alpha < -1$. Panel (d) shows $r(\alpha)$ for $\lambda = 0.08$, corresponding to the horizontal line in panel (b).

of α within the incoherent phase, for instance, $\alpha = \alpha^* = -1$, and consider the behavior of the system as we decrease the value of α. When α gets smaller than a particular critical value $\alpha_{c_1}(\lambda)$, in this case $\alpha_{c_1}(0.08) \simeq -2.0$, we observe a transition from the incoherent to the synchronized phase. Conversely, we can start at $\alpha = -1$ and get a synchronized state by increasing the motion bias parameter to values larger than $\alpha_{c_2}(0.08) \simeq -0.2$. A fine-tuning of the rules controlling the agents' motion can effectively produce dramatic changes in the *macroscopic* synchronization state of the system.

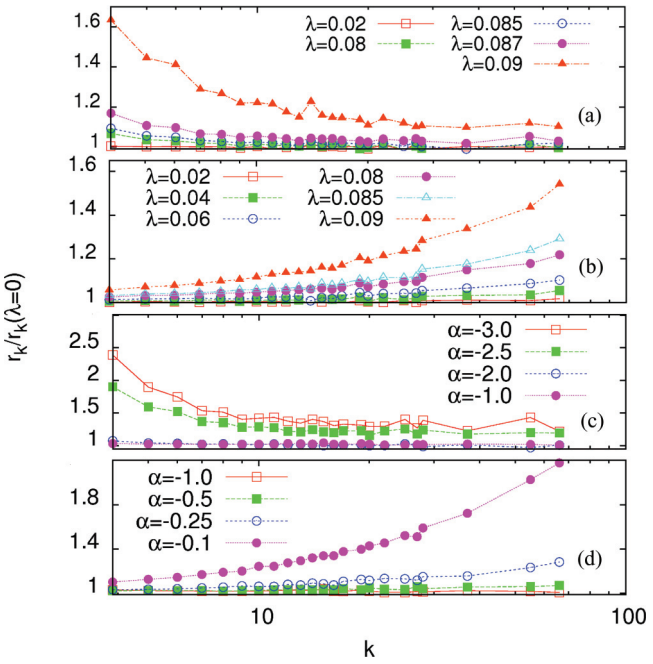

FIG. 2. (Color online) (a), (b) The average local order parameter r_k of nodes of degree k as a function of k, for various values of λ, and for two fixed values of the bias, respectively, (a) $\alpha = -2.0$ and (b) $\alpha = -0.25$, corresponding to the two vertical lines in Fig. 1(b). (c), (d) r_k for $\lambda = 0.08$ and various values of α [respectively, $\alpha < -1$ in panel (c) and $\alpha > -1$ in panel (d)] corresponding to the horizontal line in Fig. 1(b).

We have found that the bias in the motion affects the onset of synchronization also at the *microscopic* level. To illustrate this result we look at the microscopic paths to synchronization [12] as we increase λ, by following the two vertical lines shown in Fig. 1(b). In particular, we have computed the value of the local order parameter for each of the nodes of the graph, as in Eq. (4), and we have grouped nodes by degree classes. We computed the average value of the local synchronization of nodes of degree k as

$$r_k = \frac{1}{N_k}\sum_{I=1}^{N} r_I \delta(k_I,k), \tag{6}$$

where $N_k = NP(k)$ is the number of nodes of degree k. We report in Figs. 2(a) and 2(b) the quantity r_k divided by the value $r_k(\lambda \simeq 0)$ obtained when λ is close to 0 as a function of k, and for different values of λ. Figure 2(a) corresponds to $\alpha = -2.0$ and Fig. 2(b) to $\alpha = -0.25$. When $\alpha = -2.0$ the nodes having a small degree are the first ones to attain local synchronization as soon as λ crosses the critical value $\lambda_c(-2.0) \simeq 0.08$; conversely, for $\alpha = -0.25$, the hubs are the nodes which synchronize first when $\lambda > \lambda_c(-0.25) \simeq 0.07$. We thus observe two microscopic paths to synchronization: either driven by low-degree nodes ($\alpha < \alpha^*$), or by the hubs ($\alpha > \alpha^*$). The two different synchronization mechanisms are also evident by following the horizontal line in Fig. 1(b), i.e., by plotting r_k for a fixed value of λ and different values of α, as shown in Figs. 2(c) and 2(d).

B. Analytical estimation of the synchronization threshold

The effects of motion on synchronization can be explained by analytical arguments in the case of networks without degree-degree correlations. In particular we derive, as follows, a lower-bound estimate for the critical strength λ_c as a function of α. The average number w_I of biased random walkers at a node I of an undirected connected graph without degree-degree correlations reads [37,38]

$$w_I = \frac{W c_I k_I^{\alpha}}{\sum_{J=1}^{N} c_J k_J^{\alpha}} \simeq \frac{W k_I^{\alpha+1}}{\sum_{J=1}^{N} k_J^{\alpha+1}} = \frac{W k_I^{\alpha+1}}{N\langle k^{\alpha+1}\rangle}, \tag{7}$$

where $c_I = \sum_{J=1}^{N} a_{IJ} k_J^{\alpha}$. For a given α, the value w_I depends only on the connectivity k_I of the node, so that all the nodes with the same degree will have the same average number of walkers. Thus, in the following we indicate as w_k the number of agents on a node with degree k.

We consider now the two limiting cases $\Delta \to 0$ and $\Delta \to \infty$. When $\Delta \to 0$ (fast-switching approximation) the agents on a node interact for an infinitesimal time interval before moving to another node. In this limit we have a well-mixed population of oscillators that can be approximated as a single all-to-all Kuramoto model of W elements. Thus, the critical value of the coupling λ in this case reads $\Lambda_c = 2/[W \cdot \pi \cdot g(0)]$ [3,36] and does not depend on α.

When $\Delta \to \infty$ (slow-switching approximation), i.e., when the walk is much slower than the Kuramoto dynamics, each node of the network is an all-to-all Kuramoto system independent from the others. For a fixed value of λ, in some nodes the oscillators will reach local synchronization before eventually walking away, while in some other nodes they will not. In fact, the critical coupling strength of a node I is that of a set of w_I all-to-all coupled Kuramoto oscillators $\lambda_c(I) = 2/[w_I \pi \cdot g(0)]$. Hence, the critical coupling strength for the local synchronization of the walkers at a node of degree k reads

$$\lambda_c(k) = \frac{2}{w_k \pi g(0)} = \frac{4N\langle k^{\alpha+1}\rangle}{W\pi k^{\alpha+1}}, \tag{8}$$

where we have made use of Eq. (7). Therefore, in the slow-switching approximation, at fixed values of W/N, α, and λ, only agents at nodes of degree k such that $\lambda_c(k) < \lambda$ will attain local synchronization. Consequently, a necessary but not sufficient condition to have global synchronization is that there is at least one node J in the graph for which $\lambda_c(k_J) < \lambda$.

Equation (8) sheds light on the two different microscopic paths to synchronization observed in Fig. 2. Let us indicate as $k_{\min}$ and $k_{\max}$, respectively, the minimum and the maximum degrees in the network. Consider two values of α, one larger and one smaller than $\alpha^* = -1$, for instance, the two values $\alpha = -2$ and $\alpha = -0.25$ corresponding to the two vertical lines in Fig. 1(b). If we start increasing λ from $\lambda = 0$, the slow-switching approximation predicts no local synchronization until λ becomes larger than the smallest value of $\lambda_c(k)$, corresponding to $k = k_{\min}$ if $\alpha < -1$, or to $k = k_{\max}$ if $\alpha > -1$. At this point, if $\alpha < -1$ ($\alpha > -1$) the walkers at nodes with the smallest (largest) degree attain local synchronization. If we keep increasing λ, local synchronization is progressively reached also at nodes with larger (or smaller) degrees when $\alpha < -1$ (or $\alpha < -1$). We can therefore derive a lower bound $\tilde{\lambda}_c(\alpha)$ for the curve $\lambda_c(\alpha)$ delimiting the synchronization region in Fig. 1(b), by considering the smallest value of λ at which at least one class of nodes attains local synchronization. In particular, for a finite-size SF network with $P(k) \sim k^{-\gamma}$ with $\gamma \in (2,3]$, as the ones used in our simulations, we get

$$\tilde{\lambda}_c(\alpha) = \frac{4(\gamma-1)[(k_{\min})^{\gamma-1} - (k_{\min})^{\alpha+1}(k_{\max})^{\gamma-\alpha-2}]}{\pi W(\alpha+2-\gamma)}, \tag{9}$$

when $\alpha > -1$, and

$$\tilde{\lambda}_c(\alpha) = \frac{4(\gamma-1)[(k_{\max})^{\alpha+1}(k_{\min})^{\gamma-\alpha-2} - (k_{\max})^{\gamma-1}]}{\pi W(\alpha+2-\gamma)}, \tag{10}$$

for $\alpha < -1$.

We notice that if the graph is uncorrelated, a motion rule with $\alpha = -1$ leads to a uniform distribution of the walkers over the nodes since $w_I = W/N \ \forall I$ in Eq. (7), and all the nodes attain local synchronization altogether at $\lambda = 4N/(W\pi)$, as can be seen from Eq. (8). This corresponds to the largest possible value $\lambda_c^{\max}$ of the critical interaction strength. In Figs. 1(a) and 1(b) we report as a dashed line the curves $\tilde{\lambda}_c(\alpha)$ obtained for the same values of W/N, $k_{\min}$, $k_{\max}$, and γ used in the numerical simulations. Although the slow-switching approximation provides only a lower bound for the critical interaction strength, it works quite well for both kinds of SF networks, and it also predicts quite accurately the position of the cusp at $\alpha = \alpha^* = -1$ for any value of γ in $(2,3]$. In general, Eqs. (9) and (10) depend on the actual value of $k_{\min}$ and $k_{\max}$. However, power-law degree distributions with $\gamma \in (2,3]$ are characterized by unbound fluctuations, so that the value of $k_{\max}$ for scale-free random graphs having the same values of N and γ can vary in a substantial manner across different realizations. In Fig. 3 we report the theoretical predictions for $\lambda_c(\alpha)$ as a function of $k_{\max}$ obtained by Eqs. (9) and (10) for two values of

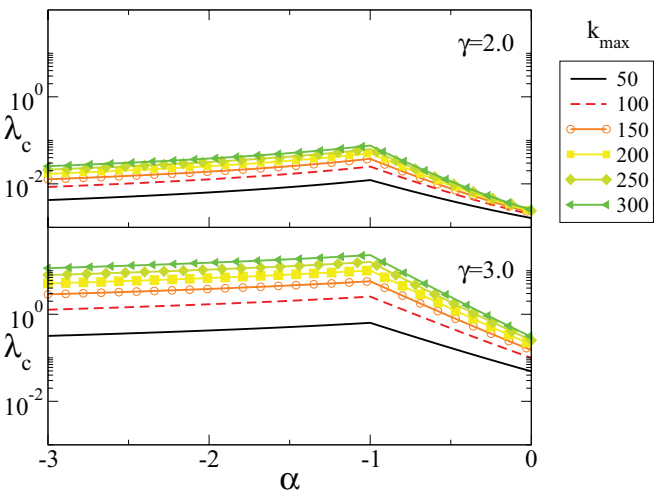

FIG. 3. (Color online) Theoretical predictions for the critical coupling strength $\lambda_c(\alpha)$ as a function of $k_{\max}$ for scale-free random graphs with exponent $\gamma = 2.0$ (top panel) and $\gamma = 3.0$ (bottom panel). When $k_{\max}$ increases, global synchronization is attained for larger values of λ. Also an increase of γ, which corresponds to more homogeneous degree distributions, produces an increase of the critical coupling strength.

γ, namely, $\gamma = 2.0$ and $\gamma = 3.0$. We observe that for fixed γ larger values of $k_{\max}$ correspond to higher values of the critical coupling $\lambda_c(\alpha)$. Moreover, by increasing γ, i.e., by moving towards more homogeneous degree distributions, the critical coupling for the onset of synchronization becomes larger. This observation confirms that degree heterogenity tends to promote global synchronization, as suggested by the phase diagrams reported in Figs. 1(a) and 1(b).

C. Interaction versus motion time scales

We now briefly discuss the impact on synchronization of the parameter Δ, which controls how often the agents perform a step of random walk. We first consider the model in the limiting case $\Delta \to \infty$, in which the agents are not allowed to move. For each value of α, we distributed a population of $W = 5000$ walkers across the nodes of a random scale-free network with $N = 500$ nodes and $P(k) \sim k^{-3}$, according to the stationary distribution of Eq. (7). Since there is no motion, each oscillator will remain at the initial node and will interact with the same set of oscillators for the duration of the simulation. In this limit, the metapopulation model is equivalent to a set of N independent all-to-all Kuramoto systems, with the system at a node of degree k having a critical interaction strength given in Eq. (8).

In Fig. 4 we report the local and global order parameters $r_{\rm loc}$ and r as a function of α and λ. We observe that, for each value of α, there exists a critical value of λ such that at least one node of the network can attain local synchronization, and by increasing λ we can reach high values of $r_{\rm loc}$ [Fig. 4(a)]. Conversely, the global order parameter r always remains close to zero, and no global synchronized state is found for any value of α and λ [Fig. 4(b)]. Notice that the phase diagram of Fig. 4(b) looks quite different from the one reported in Fig. 1(b), which corresponds to a simulation with $\Delta = 0.05$ on the same network. This indicates that, in the absence of motion, the system will remain incoherent at a global scale, even if synchronization can emerge at the level of network nodes.

The behavior of the model for $\Delta \to \infty$ is better illustrated by the cross-section plots shown in Fig. 5. Here, we report the values of local and global order parameters $r_{\rm loc}$ and r for three different choices of the bias, namely, for $\alpha = -1.5$ (black), $\alpha = -1.0$ (red), and $\alpha = -0.5$ (blue). Notice that if λ is large enough all the nodes will eventually attain local synchronization ($r_{\rm loc} \simeq 1$), but for any combination of α and λ, the system remains globally incoherent ($r \simeq 0$). As expected, all the nodes achieve full local synchronization altogether when $\alpha = -1.0$, i.e., when the system is initialized with an equal number of walkers at each node.

We now consider the metapopulation model for finite values of Δ. In Fig. 6 we report the value of the global order parameter r as a function of Δ, for $\lambda = 0.1$ and two values of the motion bias, namely $\alpha = -2.0$ (red open circles) and $\alpha = 0.5$ (blue filled circles). When the value of Δ is large, i.e., when the motion is rare with respect to the agents' interaction, the

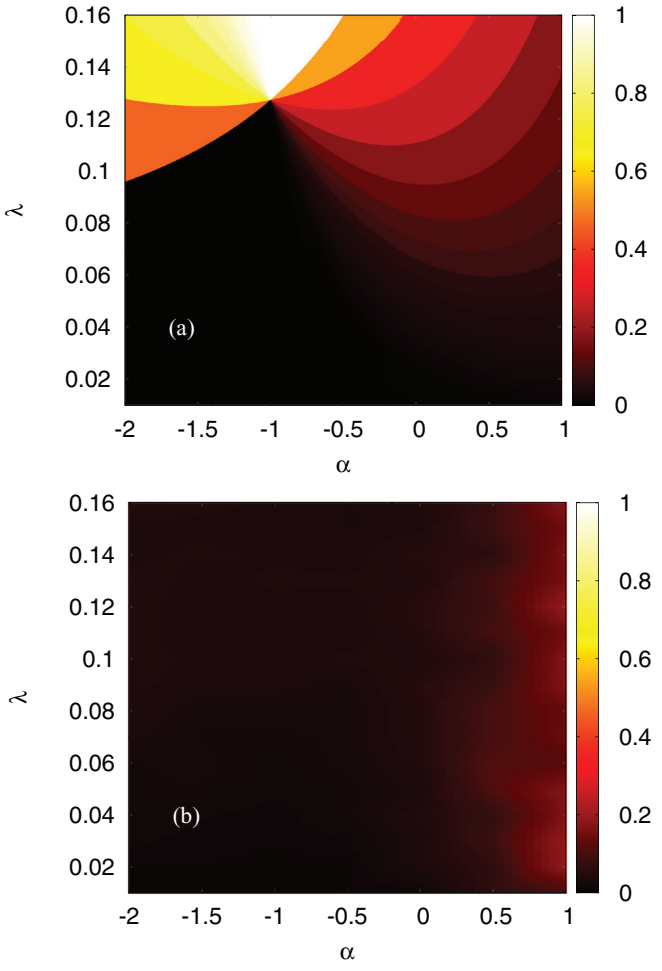

FIG. 4. (Color online) Phase diagram reporting the local and global order parameters $r_{\rm loc}$ (upper panel) and r (lower panel) as a function of α and λ for the metapopulation model in the limit $\Delta \to \infty$ ($W = 5000$ agents on a scale–free network with $N = 500$ nodes and $P(k) \sim k^{-3}$). When there is no motion, the system is globally incoherent, even if the local synchronization at the nodes can be enhanced at will by increasing the value of the interaction strength λ.

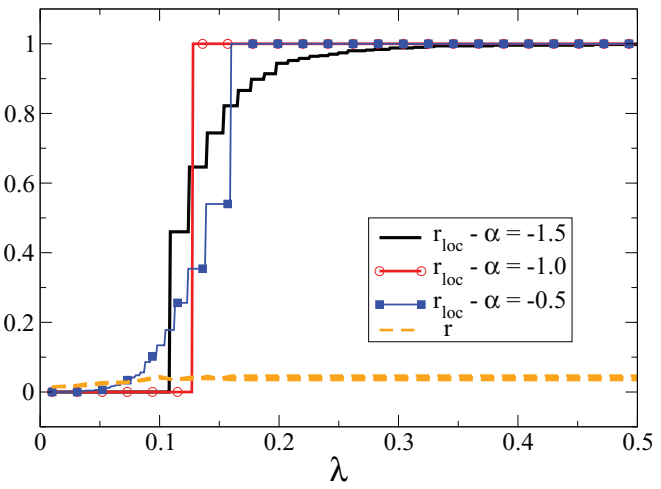

FIG. 5. (Color online) Cross-section plots of the two phase diagrams in Fig. 4. We report $r_{\rm loc}$ and r as a function of the coupling strength λ for three different values of α. The absence of motion hinders global synchronization ($r \simeq 0$, orange dashed lines), even if, for an appropriately large value of λ, all the nodes of the network can reach complete local synchronization ($r_{\rm loc} = 1$, solid lines).

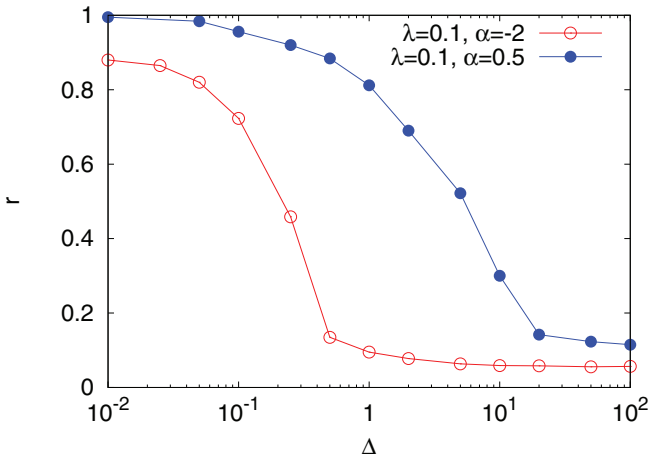

FIG. 6. (Color online) Global order parameter r as a function of Δ for $\lambda = 0.1$ and two values of the motion bias, respectively, $\alpha = -2.0$ (red open circles) and $\alpha = 0.5$ (blue filled circles). Global synchronization is attained when agents move frequently ($\Delta \to 0$), while the system remains in an incoherent state if the motion is too slow ($\Delta \to \infty$).

global order parameter decreases dramatically and approaches the behavior of the limiting case $\Delta \to \infty$. This means that even if the value of λ is large enough to guarantee that all the agents on a node will attain full synchronization between two subsequent steps of the random walk, the poor mixing due to rare motion prevents the emergence of global order. Conversely, if Δ is small then the interaction interval at each node is not large enough to allow local synchronization; nevertheless, the presence of fast motion enhances mixing and promotes the convergence of each oscillator towards a global synchronized state. The good agreement between the prediction in the slow-switching approximation and the numerical simulations reported in Fig. 1 indicates that the value $\Delta = 0.05$ corresponds indeed to an intermediate regime of the system in which the motion is fast enough to allow a sufficient mixing and the attainment of global synchronization and, at the same time, it is slow enough to avoid full mixing, for which $\lambda_c(\alpha) = \Lambda_c \ \forall \alpha$.

IV. CONCLUSION

In this work we have shown a mechanism to induce and control synchronization that is solely based on the agents' motion. To this end, we introduce and study a metapopulation model of random walkers moving over a complex network. The agents obey a one-parameter motion rule that can bias the motion either towards low-degree nodes or towards hubs. Each walker is a Kuramoto oscillator and interacts with the other oscillators present on the same node at a given time. To our knowledge, this is the first time that synchronization has been studied in a metapopulation model.

We have shown both numerically and analytically that (i) the emergence of a synchronized phase is determined by the value of the motion bias, which effectively acts as a control parameter of a motion-induced phase transition; (ii) for each fixed value of the interaction strength, there are two critical values of the motion bias, so that a fall-and-rise of synchronization can be purely driven by motion; and (iii) the two phase transitions are associated with two different microscopic paths to synchronization, respectively, driven either by hubs or by low-degree nodes.

Prior research has suggested that the strength and topology of interactions were the unique elements driving the transition from an incoherent state to synchronization. Here we prove that motion alone can control the onset of global coherence. This study paves the way towards further investigations of the interplay between mobility and synchronization in complex systems.

ACKNOWLEDGMENTS

This work has been partially supported by the Spanish MINECO Projects No. FIS2011-25167 and No. FIS2012-38266-C02-01 and the European FET project MULTIPLEX (317532). J.G.G. is supported by MINECO through the Ramón y Cajal program. V.N. acknowledges support from the EPSRC project MOLTEN (EP/l017321/1) and from the EU-LASAGNE Project, Contract No. 318132 (STREP). R.S. acknowledges support from the James S. McDonnell Foundation.

[1] A. Pikovsky, M. Rosenblum, and J. Kurths, *Synchronization: A Universal Concept in Nonlinear Sciences* (Cambridge University Press, Cambridge, England, 2003).
[2] S. Boccaletti, *The Synchronized Dynamics of Complex Systems* (Elsevier, Amsterdam, 2008).
[3] S. H. Strogatz, Physica D **143**, 1 (2000).
[4] E. Bullmore and O. Sporns, Nat. Rev. Neurosci. **10**, 186 (2009).
[5] C. Castellano, S. Fortunato, and V. Loreto, Rev. Mod. Phys. **81**, 591 (2009).
[6] A. Pluchino, V. Latora, and A. Rapisarda, Int. J. Mod. Phys. C **16**, 515 (2005).
[7] S. H. Strogatz, Nature (London) **410**, 268 (2001).
[8] S. Boccaletti, V. Latora, Y. Moreno, M. Chavez, and D.-U. Hwang, Phys. Rep. **424**, 175 (2006).
[9] A. Arenas, A. Díaz-Guilera, J. Kurths, Y. Moreno, and C. Zhou, Phys. Rep. **469**, 93 (2008).
[10] Y. Moreno and A. F. Pacheco, Europhys. Lett. **68**, 603 (2004).
[11] A. Arenas, A. Díaz-Guilera, and C. J. Pérez-Vicente, Phys. Rev. Lett. **96**, 114102 (2006).
[12] J. Gómez-Gardeñes, Y. Moreno, and A. Arenas, Phys. Rev. Lett. **98**, 034101 (2007).
[13] I. Lodato, S. Boccaletti, and V. Latora, Europhys. Lett. **78**, 28001 (2007).
[14] J. Gómez-Gardeñes, S. Gómez, A. Arenas, and Y. Moreno, Phys. Rev. Lett. **106**, 128701 (2011).
[15] T. Nishikawa, A. E. Motter, Y.-C. Lai, and F. C. Hoppensteadt, Phys. Rev. Lett. **91**, 014101 (2003).
[16] M. Chavez, D.-U. Hwang, A. Amann, H. G. E. Hentschel, and S. Boccaletti, Phys. Rev. Lett. **94**, 218701 (2005).

[17] C. Zhou, A. E. Motter, and J. Kurths, Phys. Rev. Lett. **96**, 034101 (2006).
[18] D. Gfeller and P. De Los Rios, Phys. Rev. Lett. **100**, 174104 (2008).
[19] C. Zhou and J. Kurths, Phys. Rev. Lett. **96**, 164102 (2006).
[20] F. Sorrentino and E. Ott, Phys. Rev. Lett. **100**, 114101 (2008).
[21] T. Aoki and T. Aoyagi, Phys. Rev. Lett. **102**, 034101 (2009).
[22] R. Gutierrez, A. Amann, S. Assenza, J. Gómez-Gardeñes, V. Latora, and S. Boccaletti, Phys. Rev. Lett. **107**, 234103 (2011).
[23] A. Buscarino, L. Fortuna, M. Frasca, and A. Rizzo, Chaos **16**, 015116 (2006).
[24] M. Frasca, A. Buscarino, A. Rizzo, L. Fortuna, and S. Boccaletti, Phys. Rev. Lett. **100**, 044102 (2008).
[25] N. Fujiwara, J. Kurths, and A. Díaz-Guilera, Phys. Rev. E **83**, 025101 (2011).
[26] M. Frasca, A. Buscarino, A. Rizzo, and L. Fortuna, Phys. Rev. Lett. **108**, 204102 (2012).
[27] L. Prignano, O. Sagarra, and A. Díaz-Guilera, Phys. Rev. Lett. **110**, 114101 (2013).
[28] V. Colizza, R. Pastor-Satorras, and A. Vespignani, Nat. Phys. **3**, 276 (2007).
[29] V. Colizza, A. Barrat, M. Barthélemy, and A. Vespignani, Proc. Nat. Acad. Sci. USA **103**, 2015 (2006).
[30] M. Szell, R. Sinatra, G. Petri, S. Thurner, and V. Latora, Sci. Rep. **2**, 457 (2012).
[31] V. Colizza and A. Vespignani, Phys. Rev. Lett. **99**, 148701 (2007).
[32] V. Colizza and A. Vespignani, J. Theor. Biol. **251**, 450 (2008).
[33] S. Meloni, A. Arenas, and Y. Moreno, Proc. Nat. Acad. Sci. USA **106**, 16897 (2009).
[34] S. Meloni, N. Perra, A. Arenas, S. Gómez, Y. Moreno, and A. Vespignani, Sci. Rep. **1**, 62 (2011).
[35] Y. Kuramoto, Lect. Notes Physics **30**, 420 (1975).
[36] J. A. Acebrón, L. L. Bonilla, C. J. Pérez-Vicente, F. Ritort, and R. Spigler, Rev. Mod. Phys. **77**, 137 (2005).
[37] J. Gómez-Gardeñes and V. Latora, Phys. Rev. E **78**, 065102(R) (2008).
[38] R. Sinatra, J. Gómez-Gardeñes, R. Lambiotte, V. Nicosia, and V. Latora, Phys. Rev. E **83**, 030103(R) (2011).
[39] E. A. Bender and E. R. Canfield, J. Comb. Theory, Ser. A **24**, 296 (1978).